

Bio-Based PLA Membranes for Ion Transport and Ion Filtration

M. Sriram¹, R.S. Kathirnilavan¹, K. Ashick Naina Mohammed¹, S. Ananda Kumar^{1,*}, Anshuman Mishra² and Ashutosh Tiwari²

¹Department of Chemistry, Anna University, Chennai – 600025, TN, India

²Institute of Advanced Materials, IAAM, Gammalkilsvägen 18, Ulrika 59053, Sweden

Abstract: Lithium-ion batteries require battery separators for both safety and electrochemical performance. Due to that, they have received a lot of attention. In order to prevent any electronic current from moving within the negative and positive electrodes and allow ions to flow through while avoidance of electric contact between them, a porous membrane used as a separator is positioned between the electrodes with opposing polarities. Accordingly, the objective of the present work is to build a biodegradable PLA based battery separator, which has exceptional thermal capabilities and can endure temperatures of up to 300°C. They also seem to serve as the least degree of barrier for the flow of an ionic current. In this study bio-polymer battery separator membranes were developed using PLA as matrix material and fillers such as Copper slag (CS) and Cardanol resin (CNSL). CS and CNSL were preferred for the reason to realize the concept of a wealth reclaimed from wastes that act as toughening and pore forming agent for PLA matrix. It is found that at PLA-CS film has more brittleness when compared to neat PLA and PLA-CNSL resin. On the other hand, PLA-CNSL films are the toughest ones. Overall, it has been demonstrated that obtaining more sustainable and high-performance is possible by the usage of such sustainable materials for futuristic developments.

Keywords: PLA, Bio-based Membranes, Circular Economy, Ion-filtration, Ion-transport.

1. INTRODUCTION

Recent years have seen numerous advancements in battery technology, including the creation and launch of new battery chemistries as well as the ongoing development of certain electrochemical systems, where chemical energy can be converted into electrical energy by means of electrochemical reactions in a battery [1]. A battery separator is a membrane with pores [2]. All electrochemical devices require the separator membrane, which divides the anode from the cathode. The separator's job is to act as a conduit for the ion's movement between the two electrodes and among the classes [3]. A battery separator's performance is dictated by a number of specifications, including porosity, electrical insulator, wettability, resistance to chemical reagent and electrolyte deterioration, and thermal and chemical stability [4]. Commercially available polyolefin separators are effective in reducing thermal runaway resulting from abrupt overcharging or electric short circuits because they feature great mechanical and thermal properties. Nonetheless, the hydrophobic surfaces of these separators with low surface energy impede their ability to hold onto electrolyte solutions making it hard to allow them to absorb electrolyte solvents that have high dielectric constants [5].

The sustainability problem linked to membrane production has been mitigated by the incorporation of PLA, which has led to significant advancements in preparation techniques and potential novel applications. PLA is a well-known thermoplastic polyester biopolymer that conforms to the characteristics of being

biocompatible, biodegradable, and bioresorbable [6]. In recent years, scientists are paying close attention to PLA because of its many advantages and non-toxic properties [7]. Researchers have attempted to alter PLA by modifying it using natural resources in order to alter its performance and features. Furthermore, incorporation of fillers has been proposed as a useful technique to boost and enhance PLA performance [8]. The spherulite size, degree of chain placement, crystalline thickness, crystallinity are the functional qualities that influence the attributes of PLA [9]. PLA is an elastic, stiff, hydrophilic biopolymer. This polymer offers favorable characteristics like UV resistance, excellent processing capability, thermo-plasticity, and strong mechanical properties [10]. However, PLA has drawbacks, too, including brittleness and a sluggish crystallization rate with a high crystallization temperature. These drawbacks often restrict the usage of PLA and have an impact on its production time. Accordingly, the characteristics of PLA, such as its crystallinity, is regulated by utilizing specific catalysts with syndiotactic and isotactic materials [11]. Currently, there is a growing demand for lithium-ion batteries (LIBs) fabricated with environmentally friendly materials to transition towards a more sustainable society based on a circular economy. To reduce our dependence on fossil resources, sustainable battery separators are being employed now due to their easily controllable porosity, suitable mechanical and thermal properties, non-toxicity and inherent hydrophilicity. Hence, the present work aims to research and develop a novel biocompatible and sustainable battery separator using a composite material made from polylactic acid (PLA) and Cashew nut shell liquid (CNSL) and copper slag (CS) combination.

*Address correspondence to this author at the Department of Chemistry, Anna University, Chennai – 600025, TN, India; E-mail: srinivanand@gmail.com

1.1. Development of Non-Ferrous Slag

The word "slag" refers to the entirety of non-metallic byproducts produced during the extraction of metals from their ore. The kind of metal that is melted and the smelting process have a significant impact on the chemical makeup [12]. One type of non-ferrous slag produced by melting ores is called copper slag (CS). After all, slag weighing two ton is produced for every ton of metal. Non-ferrous materials and alloys made from them are generated and consumed annually, making the handling of post-production waste an urgent problem that has to be tackled [13]. Because copper processing is so widespread, the by-product that is produced as a result generates a lot of garbage. This waste can be managed in a number of ways, but it is still useful from the perspective of waste valuation [12].

Cashew nut shell liquid (CNSL), originates from cashew nut tree, acts as an useful agricultural byproduct of the production of cashew nuts and cashew apples [14]. Various aliphatic chains containing phenolic compounds, such as cardanol and cardol comprise natural CNSL [15]. Because of its distinct chemical characteristics, CNSL can be used in a variety of ways. One of the few aromatic bio-based molecules that may be used in industrial settings at a reasonable cost is CNSL [16]. Greater thermal stability is provided by the aromatic rings in CNSL, making it suitable for use in flame-retardant materials. It is well known that CNSL's phenolic structure possesses antibacterial [17, 18] and antioxidant qualities [19, 20]. In this work, we created a new battery separator membrane, from bio-based PLA incorporated with copper slag and CNSL, to realize sustainability and waste to wealth concept.

1.2. Challenges

Regular production of wastes made of plastic and fuels contributes to the phenomenon of global warming, which is caused by the emission of greenhouse gases in every region of the world. There are only a few countries that are currently capable of recycling lithium batteries that are manufactured in mass quantities. These countries account for only five percent of the total waste that was produced in 2018, which was more than 345,000 t [21]. Additionally, a decrease in back-web thickness and a corresponding decrease in separator cost are made possible by these improvements in separator properties [22]. Furthermore, separator engineering research directions and prospects are proposed to offer a strong foundation for creating a secure and dependable battery system [23]. It's time to confront the major obstacles still standing in the way of full-scale commercialization, cell performance, and

implementation [24]. Because of thickness, mechanical strength, and practical chemical stability, polymer-based separators are widely employed. Polymer separators, in general, have pores, when the temperature of the battery rises to a point where the material in the separator melts, the holes will shut, obstructing the passage between the negative and positive electrodes and stopping the electrochemical reactions. Next-generation safe separators should have high ion-transport, strong mechanical characteristics, good thermomechanical stability, good wettability, cost-effectiveness, biodegradability, and fire resistance. Achieving all these qualities in simply one separator is a considerable task, albeit [25]. Consequently, separators with high wettability, high porosity, and strong ion conductivity should be extremely thin and suitable for large power and energy densities. It will take more work and thorough investigation to achieve the goal of acquiring such abilities and qualities.

2. MATERIALS AND METHODS

2.1. Materials

2.1.1. Poly Lactic Acid (PLA) Production

PLA polymers are made via direct lactic acid polycondensation as well as ring-opening of lactide [26] was purchased from Nature-tech India Pvt. Ltd CNSL was purchased from Sigma Aldrich, while CS was collected from Sterlite copper at Tuticorin, Tamil Nadu India and was finely milled into an average size of 25 microns using ball-milling operation.

2.2. Methods

The polymer film was casted using two different methods:

2.2.1. Solvent Casting Method

Solvent casting is one of the simplest and conventional techniques for casting polymer films using suitable solvent. This method yields polymer films based on the size of the Petri dish. PLA solution of 5% w/w is prepared by adding PLA granules with suitable organic solvent and kept stirring for magnetic stirrer at 1000rpm for almost 1 hour. Once the PLA is completely dissolved, the stock solution is poured in petri dish and film is casted. Similar procedure was followed for casting the cardanol and copper slag loaded PLA solution.

2.2.2. Phase Inversion Method

One popular technique for creating filtering membranes is phase inversion, where the polymer and solvent used has a greater influence while forming a

film, this method have four ways in, which polymer films can be prepared.

1. Temperature reduction of solution
2. Saturating polymer solution in anti-solvent
3. Exhibiting vapors of anti-solvent to the polymer solution
4. Solvent evaporation done at atmospheric condition

In this research the stock solution after being made is poured onto a glass plate and made into a film using doctor's blade. This glass plate is then immersed in water to remove the water miscible solvent and form the required porous membrane.

2.3. Instrumental Characterization

2.3.1. Fourier Transform Infrared Spectroscopy (FTIR)

Fourier Transform Infrared Spectroscopy (FTIR) is an analytical approach used to detect organic/inorganic/polymer compounds. This method mainly relies on infrared ray absorption and transmittance principle. The level of absorption/transmittance by the sample and the atomic vibration between the molecules determines the changes in chemical properties. FTIR provides basic information such as the sample's chemical composition, functional group present in it and its physical state.

2.3.2. Scanning Electron Microscopy (SEM)

Scanning electron microscopy (SEM) is a surface analyzing tool that reveals a highly magnified sample's topography. On exposing the sample with a focused electron beam and the reflected electrons are collected back and processed. This high-resolution output image is used for evaluating surface fracture and roughness or any other contaminants present over the surface.

2.3.3. Thermal Gravimetric Analysis (TGA)

Thermal Gravimetric Analysis (TGA) examines how the sample's temperature and time -related weight changes. It also determines the purity, thermal stability and material decomposition under elevated temperature conditions. This also provides a temperature range where the degradation occurs. This range provides a window for the operational temperature for a battery separator.

2.3.4. Universal Testing Machine (UTM)

Universal Testing Machine (UTM) works mainly on the principle of elongation and deformation. It's used to evaluate tensile stress and compression stress of

polymer films under various loading rate. These results are further used for calculating young's modulus.

2.3.5. Contact Angle

Contact angle measurement is quantitative measurement primarily done to evaluate the wettability of the solid substrate, which determines whether the substrate hydrophobic or hydrophilic in nature. It also determines the surface energy of solid and surface energy of liquids. Young equation is used to determine the contact angle

$$\Gamma_{SG} = \Gamma_{SL} + \Gamma_{LG} \cos \theta \quad (1.2)$$

2.3.6. Cyclic Voltammetry (CV)

The most commonly employed potentiodynamic electrochemical technique for examining the oxidation & reduction processes of molecular species is cyclic voltammetry (CV). It represents the data in form of cyclic volta-gram. This analysis provides the potential window under which a battery can work. CV works mainly on three electrode system i.e., anode (functioning electrode), cathode (counter electrode), and reference electrode.

2.3.7. Electrochemical Impedance Spectroscopy (EIS)

Electrochemical Impedance Spectroscopy (EIS) is an electrochemical analysis used to characterize electrochemical reaction mechanisms and optimize battery materials. Potentiostatic EIS refers to an EIS in which the signal being measured is current and the input signal is potential. Galvanostatic EIS is used when the input signal is current while the signal being measured is potential.

3. RESULTS AND DISCUSSION

3.1. FTIR Analysis

3.1.1. Neat PLA

FTIR spectrum of PLA granules dissolved in organic solvent is illustrated in Figure 1a. Film made of neat PLA shows characteristic peaks - 2864 cm^{-1} , 1575 cm^{-1} , 1183 cm^{-1} , 861 cm^{-1} , that represent -C-H stretching, -C=O ketone group (aliphatic polyester), COC stretching respectively, indicating the amorphous PLA. Sundar *et al.* (2021) made a similar observation [27].

3.1.2. Copper Slag

Copper slag contains FeO, SiO₂, Al₂O₃, CaO, MgO and artificially induced cellulose content. Figure 1b depicted above explains the FTIR spectrum of Copper slag containing cellulose showing characteristic peaks 3514 cm^{-1} , 2944 cm^{-1} , 2117 cm^{-1} , 1746 cm^{-1} , 954 cm^{-1} , 566 cm^{-1} , that represent hydroxyl group (O-H

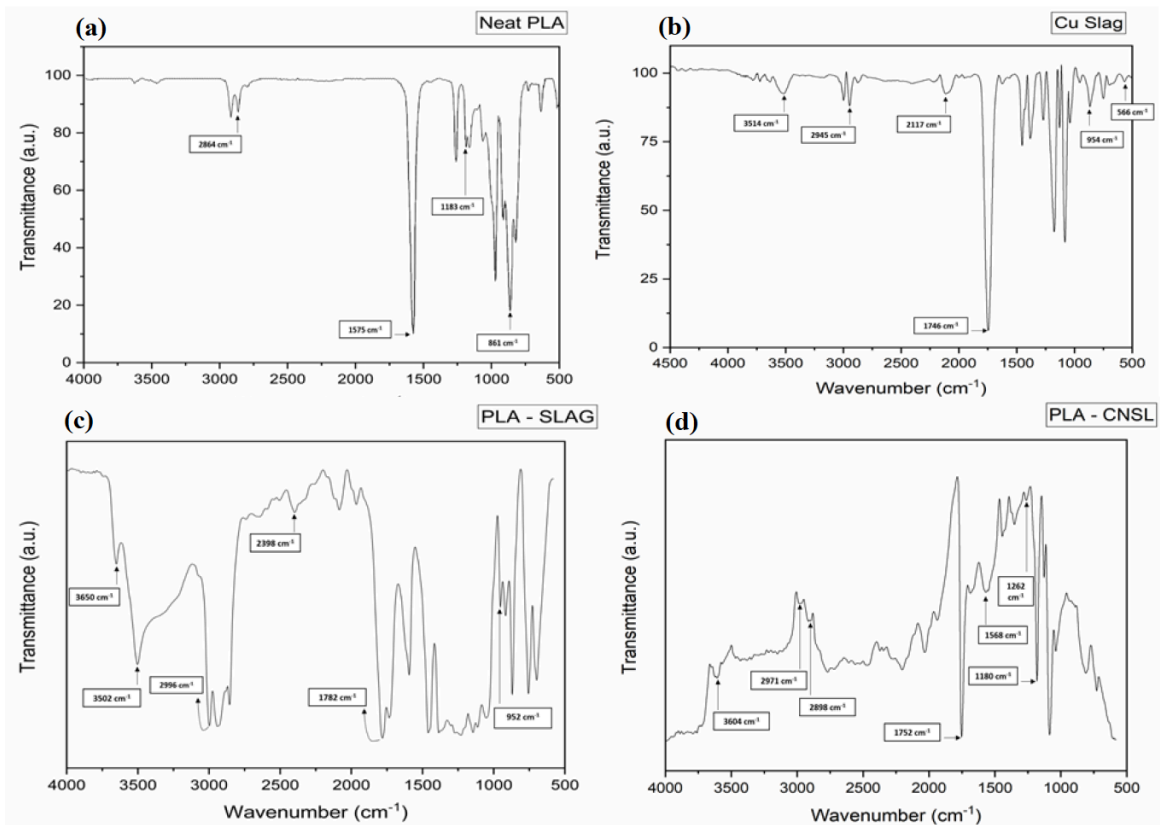


Figure 1: FTIR spectrum of (1) neat PLA, (2) Copper slag, (3) PLA-Copper slag and (4) PLA-CNSL.

stretching) intermolecular bonded cellulose (Figure 1), saturated -C-H stretching (Alkene), C \equiv C alkyne stretching, C=O stretching (Ester/ δ - lactone), traces of SiO and Al₂O₃, Fe₂O₃ respectively. Similar observation was made by I. Mihailova *et al.*, (2010) [28].

3.1.3. PLA – Slag

PLA and Copper slag of various concentrations were made and FTIR spectra obtained for 5% PLA and 5% Slag and the following characteristic peaks obtained and were shown in Figure 1c. There were about five peaks occurred at 3650 cm⁻¹, 3502 cm⁻¹, 2398 cm⁻¹, 1782 cm⁻¹ and 952 cm⁻¹. First two peaks that appear at (3650 cm⁻¹ and 3502 cm⁻¹) confirm the presence of cellulose O-H stretching and PLA thus indicating a possible interaction between PLA's C=O group and cellulose's OH group. Second peak (2398 cm⁻¹) indicates O=C=O stretching, while third peak (1782 cm⁻¹) represents carbonyl peak present in PLA and final peak (952 cm⁻¹) shows some traces of SiO₂/Al₂O₃. Similar observation was made by Mateusz Barczewski *et al.*, (2022) [29]

3.1.4. PLA – CNSL

PLA and Cardanol of various concentrations were made and FTIR spectra obtained for 10% PLA and 17% Cardanol resin was showed in Figure 1d. The characteristic peaks are obtained at 3604 cm⁻¹, 2971 cm⁻¹, 2898 cm⁻¹, 1752 cm⁻¹, 1568 cm⁻¹ and 1262 cm⁻¹. The O-H stretching peak, 3604 cm⁻¹ shows the

existence of Cardanol in PLA solution. The peaks of C-H stretching of PLA appear at 2971 cm⁻¹ & 2898 cm⁻¹. The C-H bending present in aromatic compound (i.e., Cardanol) peak corresponds to 1752 cm⁻¹ and the 1568 cm⁻¹ peak represents aromatic stretching of C=C present in Cardanol. The peak at 1262 cm⁻¹ represents the presence of aromatic ester C=O present in Cardanol. Giuseppe Mele *et al.* made a similar observation in 2019 [30].

3.2. SEM Analysis

3.2.1. PLA – Copper Slag

Figure 2a reveals the SEM image and surface topography of PLA-slag where Copper slag can be witnessed like a glossy spot. This is due to the back scattering effect of electron beam from the surface of the polymer film. Figure 2b reveals a fractured surface of neat PLA film, which indicates its brittle nature. It's understood that the incorporation of copper slag with PLA reduces the brittle behavior of PLA, which is clearly depicted in Figure 2a.

3.2.2. PLA – CNSL

The morphology of miscible mixture of PLA and Cardanol resin is depicted in Figure 3. Many possible porous topographies are quite visible, which provide a hint for the intended application namely separator plates for battery and hydrophilic membranes for water treatment. It is quite evident that the increase in

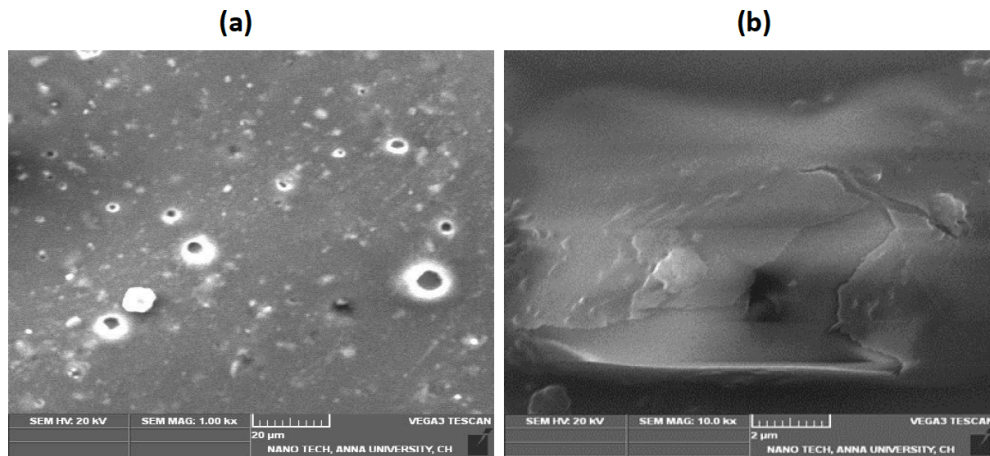


Figure 2: SEM image of (a) PLA – slag and (b) fractured PLA – slag.

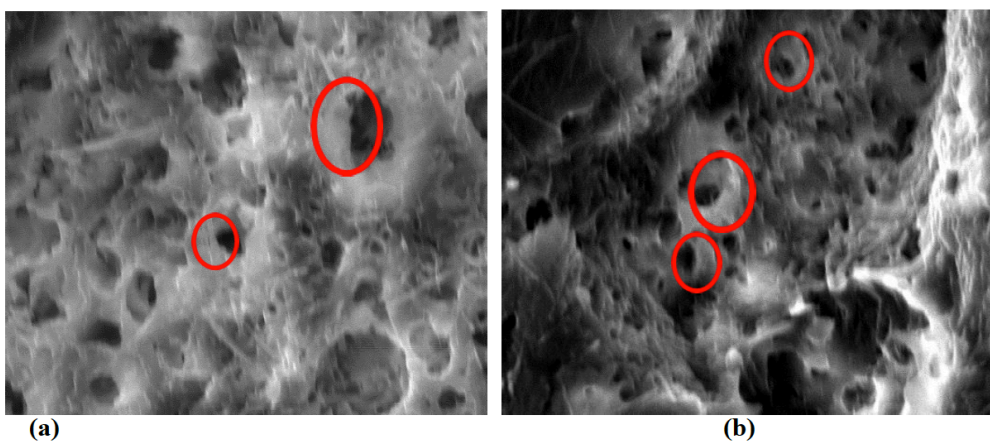


Figure 3: SEM images of PLA – CNSL.

porosity imparted by PLA - Cardanol may be due to possible interaction that occurred between the solvent (evaporated after casting) and non-solvent interaction within the mixture (PLA - Cardanol). Hence the incorporation of CNSL introduces the pores of minimum size within the separating membrane (PLA - CNSL), which are most uniformly distributed and ideally suited to facilitate the metallic particle deposition and, hence, electronic bridging. This clearly implies the suitability of PLA - CNSL membrane for the intended battery separator application.

3.3. Energy-Dispersive X-ray Spectroscopy (EDS)

Energy dispersive spectroscopy (EDS) technique is mostly used for qualitative analysis of materials which is generally equipped with SEM instrument. Figure 4, indicating the EDS of Cu slag with major composition of metal oxides namely Fe_2O_3 , SiO_2 , CaO , Al_2O_3 as observed in Aleksander Hejna *et al.*, (2021). Since the percentage of oxygen is comparatively higher, therefore we may conclude that metal oxides have a major composition in Cu slag. Interestingly, none of these above-mentioned elements have not been reported as they promote biocidal activity that restricts enzymatic biodegradation of a matrix in the later stages.

This is the prime reason for preferring Cu slag as a filler material with PLA.

3.4. TGA Analysis

3.4.1. PLA-Slag

Thermogram obtained in Figure 5a indicating PLA-Slag onset degradation temperature (T_{onset}). The film sample is heated under inert condition (N_2) at a temperature range of 30–700°C. Based on the sample temperature vs weight loss percentage its first derivative (dTG) curve is obtained. Thermogram obtained in Figure 5a indicates PLA-Slag onset degradation temperature (T_{onset}) ranging from 300°C and complete degradation occurs around 600°C. This single-step degradation process initiates around 150°C. The filler (Cu slag), which is finely milled and added to the matrix might enhance the thermal stability of the film since Cu slag majorly composed of metal oxides (refer Figure 5a). All those metal oxides are generally non-conductive and stable under hot conditions hence the thermal emissivity of the filler is comparatively low thus enhancing the safety of the battery by restricting the thermal runaway reaction. For PLA-Slag the T_{onset} value significantly exceeds the thermal stability

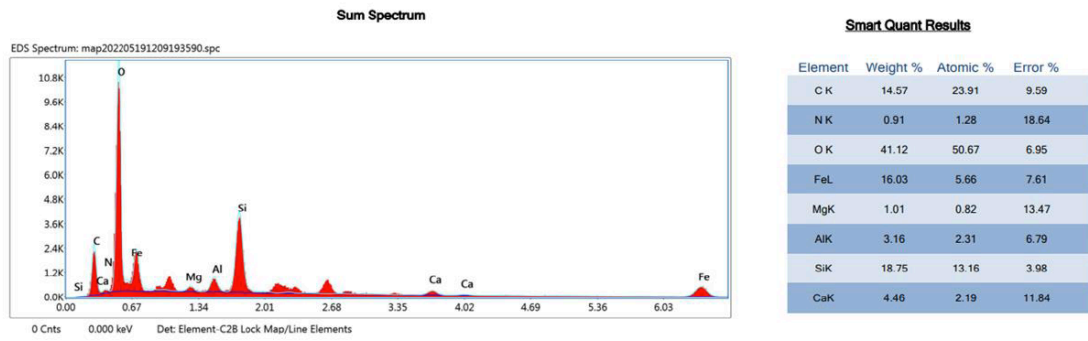


Figure 4: EDS spectrum-Copper slag.

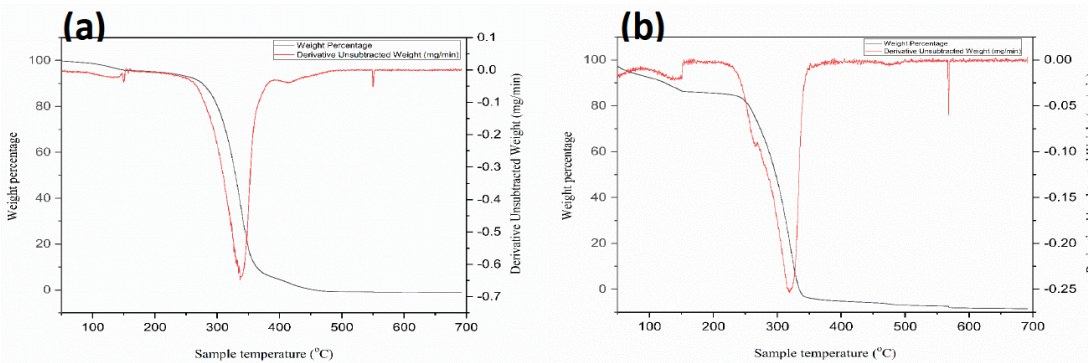


Figure 5: TGA and DTG curve for (a) PLA-Slag and (b) PLA – CNSL.

temperature for the intended application. Therefore, it shows that a battery separator would be appropriate given the observed thermal stability.

3.4.2. PLA-CNSL

Thermogram obtained in Figure 5b indicating PLA-CNSL onset degradation temperature (T_{onset}). The film sample is heated under inert condition (N₂) at a temperature range of 30-700°C. Based on the sample temperature vs weight loss percentage its first derivative (dTG) curve is obtained. Thermogram obtained in Figure 5b indicates PLA-CNSL onset degradation temperature (T_{onset}) ranging from 250°C and complete degradation occurs around 600°C. The thermal stability of the PLA-CNSL combination may be due to the presence of phenolic group (resonance stable) followed with a long pendant group (C₆H₅OH-C₁₅H₂₅₋₃₁) in the meta position since cardanol boils around 225°C it possess a good thermal stability.

3.5. UTM Analysis

3.5.1. PLA-Slag

Films made using PLA and Cu slag combination are cut into the required size and preconditioned. Figure 6a indicating force vs extension graph which is obtained from the UTM. Tensile stress, Tensile strain and young’s modulus are calculated based on the equation 1.3, 1.4 and 1.5 respectively.

$$\text{Tensile stress } (\sigma) = \frac{63.308}{25 \times 0.172} = 14.723 \text{ N/mm}^2$$

$$\text{Tensile strain } (\epsilon) = \frac{1.338}{70} = 0.019$$

$$\text{Young’s modulus } (E) = \frac{14.72}{0.019} = 774.737 \text{ MPa}$$

The variation in tensile strength may be due to the presence of cellulose in copper slag where it has a linear extended structure without any branches hence there’s an increase in mechanical property for this combination.

3.5.2. PLA-CNSL

Films made using PLA and CNSL slag combination are cut into the required size and preconditioned. Figure 6b indicating force vs extension graph which is obtained from the UTM. Tensile stress, Tensile strain and young’s modulus are calculated based on the equation 1.3, 1.4 and 1.5 respectively.

$$\text{Tensile stress } (\sigma) = \frac{21.327}{25 \times 0.034} = 25.090 \text{ N/mm}^2$$

$$\text{Tensile strain } (\epsilon) = \frac{1.725}{70} = 0.025$$

$$\text{Young’s modulus } (E) = \frac{25.090}{0.025} = 1003.600 \text{ MPa}$$

This increase in tensile strength may be due to the reduction in brittleness of PLA by addition of CNSL where an aliphatic ester group combined with a phenol attached with a long pendant side group which provides a longer chain length thereby increase in tensile strength is observed.

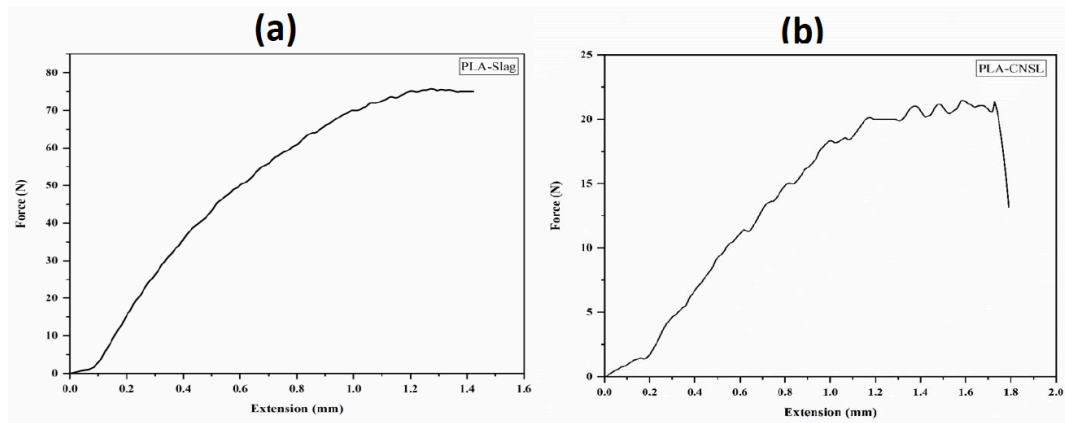


Figure 6: Force vs Extension of (a) PLA – Slag and (b) PLA-CNSL.

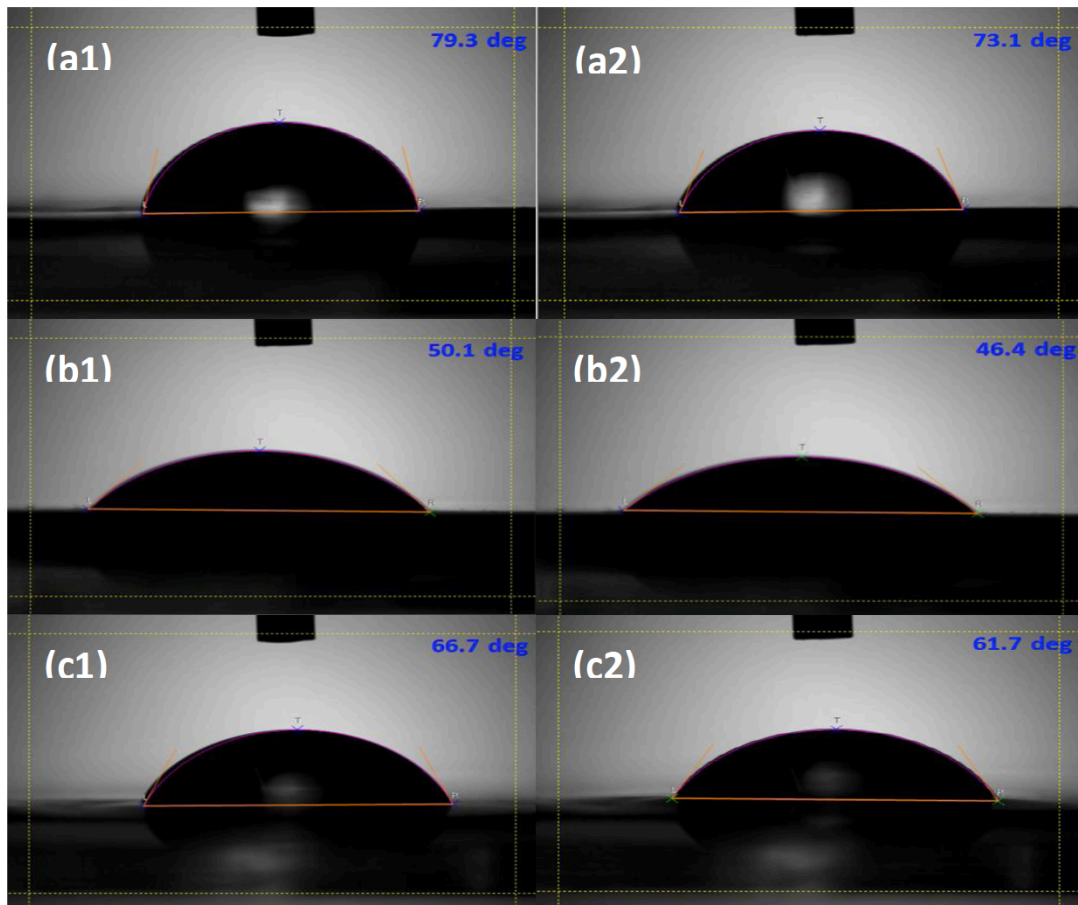


Figure 7: Contact angle of neat PLA (a1) 0 min and (a2) 5 min, PLA – Slag (b1) 0 min and (b2) 5 min, PLA – CNSL (c1) 0 min and (c2) 5 min.

3.6. Contact Angle

3.6.1. Neat PLA

PLA films made with stoichiometric weight percentage is placed in the slit with size of 1.5cm x 1.5cm and the inferred contact angle images are given in Figure 7a1 and a2. The contact angle images clearly indicating that the films made using neat PLA are comparatively hydrophobic in nature. This hydrophobic nature is primarily due to lack of interactive site for the molecules of water on the surface of the PLA and the hydrophobic interaction between the two phases.

3.6.2. PLA-Slag

Films casted with PLA and Cu slag as filler material were cut into sizes of 1.5cm x 1.5cm are used. The observed contact angles are indicated in Figure 7b1 and b2.

Interestingly on addition of Cu slag the contact angle getting reduced drastically as the water droplet moves towards the spreading front as time progresses this may be because of the carbonyl and hydroxyl groups found in the repeating units of cellulose. Each cellulose unit contains a hydroxyl group linked to it in

the anhydro glucose unit at positions 2, 3, and 6, which forms hydrogen bonds between and within molecules. This reduction in contact angle promotes a good wettability of electrolytes for the separator application.

3.6.3. PLA-CNSL

Film samples made out using PLA and CNSL are cut to the required dimension and contact angle is measured and depicted in Figure 7c1 and c2. On the addition of CNSL the contact angle getting reduced upto some extent this may be due to the OH group present in the CNSL but cardanol based liquids contains lipophilic C₁₅ chains which are partially soluble in water.

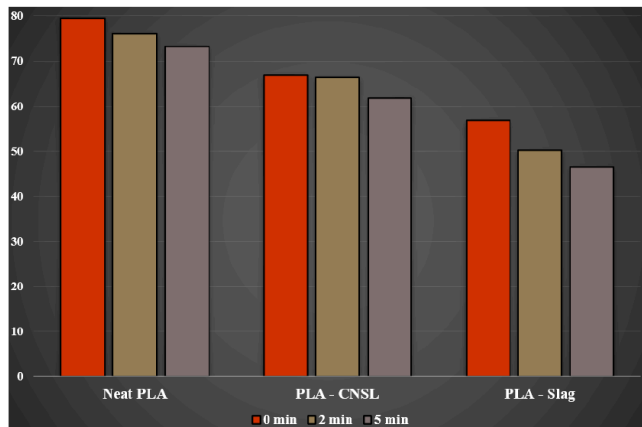


Figure 8: Comparative study of contact angle.

Figure 8 shows the comparative study of all the observed contact angle, where it's quite evident that the contact angle is gradually getting reduced with respect to time which promotes a better wettability surface at an ascending order starting from neat PLA, PLA-CNSL and PLS-Slag.

3.7. Water Uptake

Film samples are cut into appropriate sizes and conditioned in hot air oven at 105± 2° C for 12hours. After removing any remaining water on the film surface, the sample is weighed and immersed within distilled water about a day.

$$\text{Moisture content (\%)} = \frac{w_2 - w_1}{w_1} \times 100$$

W₁ = Film - dry weight

W₂ = Film – wet weight

Neat PLA

$$\text{Moisture content (\%)} = \frac{0.02 - 0.018}{0.018} \times 100 = 11.11\%$$

PLA-Slag

$$\text{Moisture content (\%)} = \frac{0.034 - 0.011}{0.011} \times 100 = 209.09\%$$

PLA-CNSL

$$\text{Moisture content (\%)} = \frac{0.04 - 0.034}{0.034} \times 100 = 176.47\%$$

From the above observed results it is quite evident that the combination PLA-Slag have better uptake value.

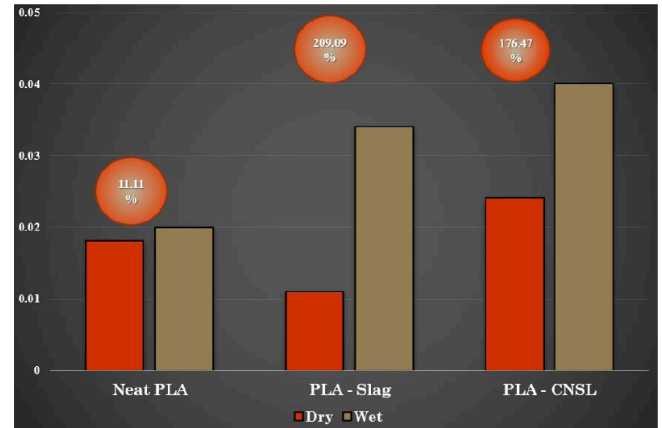


Figure 9: Comparative study of water uptake.

3.8. Electrolyte Stability

Films made out using PLA with Cu slag and CNSL must be stable in electrolytes which acts as a medium for ions transportation. Hence, H₂SO₄ is prepared at various concentrations ranging from 1M, 2M, 3M, 4M, 5M, 6M and polymer films are preconditioned to remove the moisture content, placed in separate test tubes to determine its stability at different concentrations.

$$\text{Weight loss/gain (\%)} = \frac{w_2 - w_1}{w_1} \times 100$$

W₁ = Film - dry weight

W₂ = Film – wet weight

Neat PLA

$$\text{Weight loss/gain (\%)} = \frac{0.0196 - 0.018}{0.018} \times 100 = 8.88\%$$

PLA-Slag

$$\text{Weight loss/gain (\%)} = \frac{0.023 - 0.019}{0.019} \times 100 = 21.05\%$$

PLA-CNSL

$$\text{Weight loss/gain (\%)} = \frac{0.023 - 0.019}{0.019} \times 100 = 26.66\%$$

3.9. NAOH DEGRADATION

PLA based films mainly composed of aliphatic polyester backbone, the prime objective of this separator is to degrade in sustainable manner. Hence, NaOH degradation is performed to analyze the complete degradation time. Polymer films made using PLA-Slag/CNSL were preconditioned and immersed in

0.1M NaOH solution for a month and weighed for each 10 hours to check the degradability of the films.

From Figure 10, it is quite evident that the neat PLA film gets degraded around 71 hours, which may be due to its cleaving of ester bond at pH of 13. However, PLA-Slag based film gets degraded around 92 hours. Interestingly a delay in degradation occurs due to the swelling nature of the OH group and the metal oxides present in the slag, thereby reducing the rate of degradation. In contrast, PLA-CNSL based films underwent a rapid degradation and gets degraded around 80 hours (which fall in between the degradation of PLA-Slag and neat PLA). This is because of the phenolic OH group that exists in cardanol, which is slightly acidic in nature and gets neutralized easily with a basic medium.

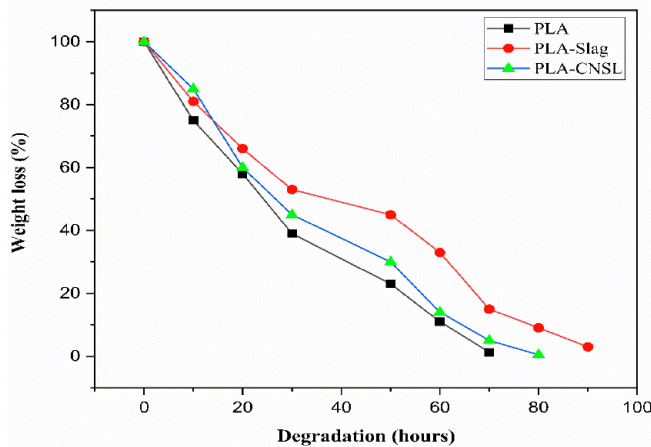


Figure 10: Weight loss due to NaOH.

3.10. Cyclic Voltammetry

Cyclic voltammetry performed to analyze the potential range where there will be no faradic reaction undergoes, which indicates that the polymer film and electrolyte are stable under such voltage conditions.

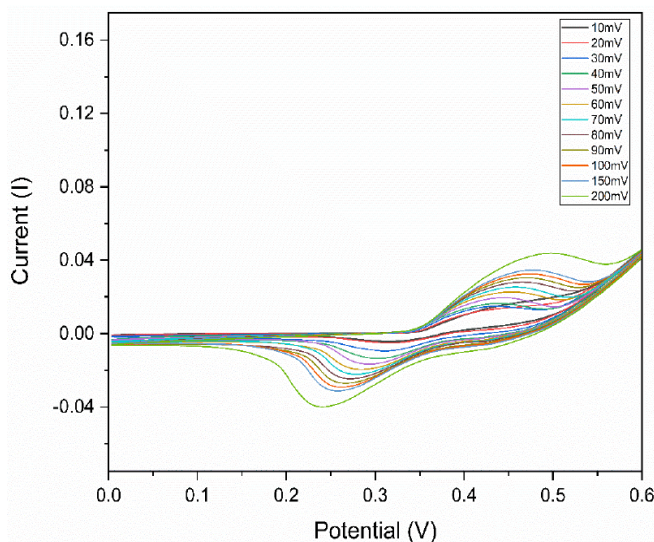


Figure 11: Cyclic voltammogram.

Table 1: Electrode Setup for CV

Working electrode (anode)	PLA-Slag/CNSL
Counter electrode (cathode)	Platinum wire
Reference electrode	Ag/AgCl
Electrolyte	1M H ₂ SO ₄

From the Figure 11, the obtained voltammogram represents the potential window for the given electrochemical cell setup. Potential window obtained here is 0.2 to 0.6 V in the range, this indicating the setup's operational voltage.

3.11. Electrochemical Impedance Spectroscopy (EIS)

EIS, the commonly used method to analyze the impedance of polymer films and to evaluate the ionic conductance using a three-electrode system. Film samples are cut in the shape of 'T' section with the flange section area of 1 cm².

Table 2: Electrode Setup for EIS

Working electrode (anode)	PLA-Slag/CNSL
Counter electrode (cathode)	Graphite
Reference electrode	Ag/AgCl
Electrolyte	1M H ₂ SO ₄

From the given plot in Figure 12, bulk resistance (R_b) can be inferred from the red-coloured dotted circle, which actually indicates the state of health (SOH) of a battery. R_b value is influenced by depletion of electrolyte and formation of microporous cracks. Generally, with the help of R_b we can determine the flaws in the separator (greater the R_b higher will be the microporous cracks).

$$\text{Ionic conductivity, } \sigma = \frac{t}{R_b A}$$

Where t being thickness of film sample and A is the film's cross-sectional area.

4. INDUSTRIAL PERSPECTIVE AND FUTURE PROSPECT

Reinforcements are used to improve these features by improving their wear, corrosion, mechanical, and thermal behavior. This in turn makes the material suitable for a wider range of applications, including those in the automotive and biomedical industries, which are made possible through the development of battery separators. Polymer materials have electrochemical, sensor and biodegradable properties [31-33].

Its popularity as a choice for PLA-based bio-composite can be ascribed to several factors,

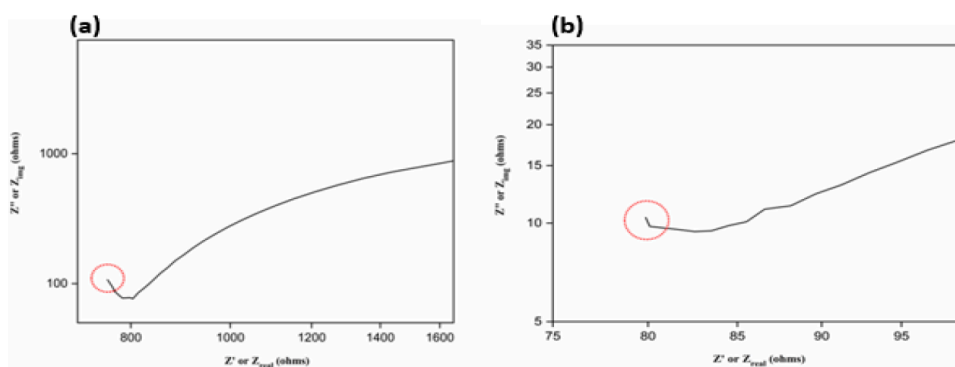


Figure 12: Nyquist plot for (a) PLA-Slag and (b) PLA-CNSL.

Table 3: Ionic Conductivity

Parameter	PLA-Slag	PLA-CNSL
Thickness (t)	0.0102 cm	0.0031 cm
Bulk resistance (R_b)	759.256 Ω	79.875 Ω
Area of sample (A)	1 cm ²	1 cm ²
Ionic conductivity (σ)	0.01 mS/cm	0.038 mS/cm

including its ease of low density, accessibility, low price, strong acoustic and thermal insulation, recyclability, eco-friendliness, adequate mechanical properties and renewability. The building and construction sector, the packaging sector, the transportation sector, the military, the sporting equipment industry, and the medical industry are all currently using natural fiber-based polymer composites to reduce greenhouse gas emissions.

In 2021, 33% of the world's bioplastics were made of PLA, a semi-crystalline bioplastic that is both lightweight and one of the most popular biopolymers [34]. While PLA breaks down in living organisms, it may however, take longer for it to dissolve in water and other naturally occurring environments. The exposed biota may be in grave danger because polylactic acid breaks down into microplastics more quickly than plastics made from petroleum [31]. It can be mixed with different substances or polymers to 3D printing, biomedical packaging, and bio-separator by modifying properties. Without a doubt, these composites and blends of PLA will provide the industries with both economic and ecological support [35]. Further investigation is needed in this field to enhance, mechanical properties of different composites based on PLA. The research should include, addition of different fabrication methods, reinforcements and energy projects. The battery industry is expected to produce energy products that are climate neutral as a result of innovative approaches.

5. CONCLUSIONS

Bio-polymer membranes were developed using PLA as matrix material and fillers such as CS and

CNSL resin were preferred for the reason to realize the concept of wealth reclaimed from a waste as toughening and pore forming agent for PLA matrix. It's found that at PLA-CS film has more brittleness when compared to neat PLA and PLA-Cardanol resin. On the other hand, PLA-CNSL films are the toughest one. Incorporation of CNSL introduces pores of minimum size within the separating membrane (PLA-CNSL), which are most uniformly distributed and ideally suited to enable the transport of ions, leading to electrical conductance and bridging. Furthermore, the data obtained from different study clearly indicate that CS waste may be used as toughening agent for PLA and CNSL can be used as pore forming agent for PLA to enable its application for bio-based membranes that can be explored for both ion transport in battery separator and ion filtration in water treatment application as well.

ACKNOWLEDGEMENT

We are thankful to the DST-FIST sponsored Department of Chemistry Anna University for providing Instrumentation facilities to our research work.

REFERENCES

- [1] Costa CM. Polymer composites and blends for battery separators: State of the art, challenges and future trends. *Journal of Power Sources* 2015; 281. <https://doi.org/10.1016/j.jpowsour.2015.02.010>
- [2] Arora P, Zhang Z. Battery separators. *Chemical Reviews* 2004; 104(10): 4419-4462. <https://doi.org/10.1021/cr020738u>
- [3] Costa CM, Silva M, Costa CM, Miguel C, Silva MM. RSC Advances polymers and copolymers for lithium ion battery transfer of the lithium ions between both electrodes and to and their application in the. *RSC Advances* 2013; pp. 11404–11417. <https://doi.org/10.1039/c3ra40732b>
- [4] Barbosa C. Recent Advances in Poly (vinylidene fluoride) and Its Copolymers for Lithium-Ion Battery Separators. *Membranes*. <https://doi.org/10.3390/membranes8030045>

- [5] Kim JY, Lim DY. Surface-modified membrane as a separator for lithium-ion polymer battery. *Energies* 2010; 3(4): 866-885. <https://doi.org/10.3390/en3040866>
- [6] Bishai M, De S, Adhikari B, Banerjee R. A comprehensive study on enhanced characteristics of modified polylactic acid based versatile biopolymer. *European Polymer Journal* 2014; 54: 52-61. <https://doi.org/10.1016/j.eurpolymj.2014.01.027>
- [7] Vatanpour V, Teber OO, Mehrabi M, Koyuncu I. Polyvinyl alcohol-based separation membranes: a comprehensive review on fabrication techniques, applications and future prospective. *Materials Today Chemistry* 2023; 28: 101381. <https://doi.org/10.1016/j.mtchem.2023.101381>
- [8] Vatanpour V, Dehqan A, Pazireh S, Zinadini S, Akbar A, Koyuncu I. Polylactic acid in the fabrication of separation membranes: A review. *Separation and Purification Technology* 2022; 296.
- [9] Farah S, Anderson DG, Langer R. Physical and mechanical properties of PLA, and their functions in widespread applications — A comprehensive review. *Advanced Drug Delivery Reviews* 2016; 107: 367-392. <https://doi.org/10.1016/j.addr.2016.06.012>
- [10] Zhao X. Super tough poly (lactic acid) blends. *RSC Advances* 2020; pp. 13316–13368. <https://doi.org/10.1039/d0ra01801e>
- [11] Mundargi RC, Babu VR, Rangaswamy V, Patel P, Aminabhavi TM. Nano / micro technologies for delivering macromolecular therapeutics using poly (D, L -lactide- co -glycolide) and its derivatives. *Journal of Controlled Release* 2008; 125: 193-209. <https://doi.org/10.1016/j.jconrel.2007.09.013>
- [12] Murari K, Siddique R. Use of waste copper slag, a sustainable material. *Journal of Material Cycles and Waste Management* 2015; pp. 13-26. <https://doi.org/10.1007/s10063-014-0254-x>
- [13] Gorai B, Jana RK. Characteristics and utilisation of copper slag: A review. *Resources, Conservation and Recycling* 2003; 39. [https://doi.org/10.1016/S0921-3449\(02\)00171-4](https://doi.org/10.1016/S0921-3449(02)00171-4)
- [14] Lucilia M. Utilisation of Cashew Nut Shell Liquid from *Anacardium occidentale* as Starting Material for Organic Synthesis: A Novel Route to Lasiodiplodin from Cardols Maria Lucilia dos Santos, and Gouvan C. de Magalhães. *Journal of the Brazilian Chemical Society* 1999; 10(1): 13-20. <https://doi.org/10.1590/S0103-50531999000100003>
- [15] Gedam PH, Sampathkumaran PS. Contents 1. *Progress in Organic Coatings* 1986; 14: 115-157. [https://doi.org/10.1016/0033-0655\(83\)85006-7](https://doi.org/10.1016/0033-0655(83)85006-7)
- [16] Sultania M, Rai JSP, Srivastava D. Process modeling, optimization and analysis of esterification reaction of cashew nut shell liquid (CNSL) -derived epoxy resin using response surface methodology. *Journal of Hazardous Materials* 2011; 185(2-3): 1198-1204 <https://doi.org/10.1016/j.jhazmat.2010.10.031>
- [17] Rodrigues FHA, Feitosa JPA, Ricardo NMPS. Antioxidant Activity of Cashew Nut Shell Liquid (CNSL) Derivatives on the Thermal Oxidation of Synthetic. *Journal of the Brazilian Chemical Society* 2006; 17(2): 265-271. <https://doi.org/10.1590/S0103-50532006000200008>
- [18] Mazzeo SE. Thiophosphate esters of cashew nutshell liquid derivatives as new antioxidants for poly (methyl methacrylate). *Journal of Thermal Analysis and Calorimetry* 2011; pp. 1177-1183. <https://doi.org/10.1007/s10973-011-1404-1>
- [19] Kim YH, An ES, Song BK, Kim DS, Chelikani R. Polymerization of cardanol using soybean peroxidase and its potential application as anti-biofilm coating material. *Biotechnology Letters* 2003; 20: pp. 1521-1524. <https://doi.org/10.1023/A:1025486617312>
- [20] Hoon Y, Chul J, Keun J, Young S, Hyun D, Lee T. Anti-biofouling behavior of natural unsaturated hydrocarbon phenols impregnated in PDMS matrix. *Journal of Industrial and Engineering Chemistry* 2008; 14: 292-296. <https://doi.org/10.1016/j.jiec.2008.01.012>
- [21] Melchor-Martínez EM, Macías-Garbett R, Malacara-Becerra A, Iqbal HMN, Sosa-Hernández JE, Parra-Saldivar R. Environmental impact of emerging contaminants from battery waste: A mini review. *Case Studies in Chemical and Environmental Engineering* 2021; 3: 100104. <https://doi.org/10.1016/j.csee.2021.100104>
- [22] Böhnstedt W. Challenges for automotive battery separator development. *Journal of Power Sources* 1997; 67(1-2): 299-305. [https://doi.org/10.1016/S0378-7753\(97\)02560-3](https://doi.org/10.1016/S0378-7753(97)02560-3)
- [23] Choi J, Kim PJ. A roadmap of battery separator development: Past and future. *Current Opinion in Electrochemistry* 2022; 31: 100858. <https://doi.org/10.1016/j.coelec.2021.100858>
- [24] Janek J, Zeier WG. Challenges in speeding up solid-state battery development. *Nature Energy* 2023; 8: 230-240. <https://doi.org/10.1038/s41560-023-01208-9>
- [25] Ely TO, Kamzabek D, Chakraborty D. Batteries Safety: Recent Progress and Current Challenges. *Frontiers in Energy Research* 2019; 7. <https://doi.org/10.3389/fenrg.2019.00071>
- [26] Angelin Swetha T, Ananthi V, Bora A, Sengottuvelan N, Ponnuchamy K, Muthusamy G, Arun A. A review on biodegradable polylactic acid (PLA) production from fermentative food waste - Its applications and degradation. *International Journal of Biological Macromolecules* 2023; 234: 123703. <https://doi.org/10.1016/j.ijbiomac.2023.123703>
- [27] Sundar N, Stanley SJ, Kumar SA, Keerthana P, Kumar GA. "Development of dual purpose, industrially important PLA-PEG based coated abrasives and packaging materials. *Journal of Applied Polymer Science* 2021; 138(21): 1-18 <https://doi.org/10.1002/app.50495>
- [28] Mihailova I, Mehandjiev D. Characterization of fayalite from copper slags. *Journal of the University of Chemical Technology and Metallurgy* 2010; 45(3): 317-326. [Online]. Available: <https://www.researchgate.net/publication/256503470>
- [29] Barczewski M, *et al.* Rotational molding of polylactide (PLA) composites filled with copper slag as a waste filler from metallurgical industry. *Polymer Testing* 2022; 106. <https://doi.org/10.1016/j.polymertesting.2021.107449>
- [30] Mele G, *et al.* Influence of Cardanol Oil on the Properties of Poly(lactic acid) Films Produced by Melt Extrusion. *ACS Publications* 2019; 4(1): 718-726 <https://doi.org/10.1021/acsomega.8b02880>
- [31] Tiwari A, Gong S. Electrochemical detection of a breast cancer susceptible gene using cDNA immobilized chitosan-co-polyaniline electrode. *Talanta* 2009; 77(3): 1217-1222. <https://doi.org/10.1016/j.talanta.2008.08.029>
- [32] Tiwari A, Singh V. Synthesis and characterization of electrical conducting chitosan-graft-polyaniline. *Express Polymer Letters* 2007; 1(5): 308-317. <https://doi.org/10.3144/expresspolymlett.2007.44>
- [33] Tiwari A, Graier JJ, Pilla S, Steeber DA, Gong S. Biodegradable hydrogels based on novel photopolymerizable guar gum-methacrylate macromonomers for in situ fabrication of tissue engineering scaffolds. *Acta Biomaterialia* 2009; 5(9): 3441-3452. <https://doi.org/10.1016/j.actbio.2009.06.001>
- [34] Ali W, Ali H, Gillani S, *et al.* Polylactic acid synthesis, biodegradability, conversion to microplastics and toxicity: a review. *Environmental Chemistry Letters* 2023; 21: 1761-1786. <https://doi.org/10.1007/s10311-023-01564-8>
- [35] Sreekumar K, Bindhu B, Veluraja K. Perspectives of polylactic acid from structure to applications. *Polymers from Renewable Resources* 2021; 12(1-2): 60-74. <https://doi.org/10.1177/20412479211008773>

Received on 22-10-2023

Accepted on 26-11-2023

Published on 27-12-2023

<https://doi.org/10.6000/1929-5995.2023.12.21>© 2023 Sriram *et al.*; Licensee Lifescience Global.

This is an open-access article licensed under the terms of the Creative Commons Attribution License (<http://creativecommons.org/licenses/by/4.0/>), which permits unrestricted use, distribution, and reproduction in any medium, provided the work is properly cited.